Scalable active acoustic metamaterials with programmable bulk modulus and mass density tensor

Dylan A. Kovacevich and Bogdan-Ioan Popa

Department of Mechanical Engineering, University of Michigan, Ann Arbor, Michigan 48109, USA

ABSTRACT

Passive acoustic metamaterials are constrained in their achievable properties and ability to integrate into realizable devices by unwanted property coupling, narrowband resonance, high loss, and challenges of fabrication. These limitations can be overcome by instead employing active components, such as speakers and microphones, to generate the desired acoustic response. We have developed an approach to designing scalable active metamaterials that allows for each unit cell to be of identical hardware and independent programming, but interact together as a bulk medium with desired effective properties. Unlike in a controls approach, the programming of these unit cells is a simple gain between local sensor and driver components. Here, we demonstrate an active metamaterial with individually programmable bulk modulus and mass density tensor. We validate its effective properties by comparing its experimental scattering behavior to that of simulated continuous media.

Keywords: Acoustics, active metamaterials, transformation acoustics, bulk modulus, mass density

1. INTRODUCTION

Transformation acoustics and other similar design strategies for devices featuring extreme sound wave manipulation have increased the demand for materials with acoustic properties beyond those that are conventionally available. The primary approach to satisfying this demand has been the development of metamaterials, which consist of periodic subwavelength architectures [1,2]. At highly subwavelength unit cell sizes, these metamaterials behave in a manner that is acoustically identical (i.e., they produce the same scattered fields) as continuous media and they can be homogeneously characterized by the effective properties of bulk modulus κ_{eff} and mass density $\boldsymbol{\rho}_{\text{eff}}$. In principle, metamaterial unit cells can be designed for desired effective properties and arranged in space to satisfy an arbitrary property map, but this is challenging in practice.

Metamaterials composed of resonant structures have been of great interest because their effective properties can vary widely from those of their constituent materials, even into the negative regime [3,4]. But for practical applications, broadband functionality is typically required and resonant structures only perform well in a narrow frequency range. There has been some success in realizing transformation acoustics devices using non-resonant passive metamaterials, such as in the case of the cloak [5,6]. However, significant simplifications to the material property specifications were necessary and the narrow channel structures that were used led to high loss, both degrading performance.

Alternatively, active acoustic metamaterials that use powered driver elements to directly produce a response to the locally sensed field are not inhibited by the physical constraints of passive metamaterials, broadening the range of achievable effective properties and bandwidth. Experimental demonstrations have shown the capability to program the acoustic bulk modulus [7,8], mass density [7–9], and Willis parameters [10,11]. Similar results were also shown for elastic waves [12,13]. The appropriate scattering behavior for a unit cell can be accomplished through various programming strategies that relate the driver outputs to the sensor inputs. Some examples are feedback control, the mimicking of resonance, or our strategy of interest, simple gains between the sensing and driving components. Past active acoustic metamaterial experimental demonstrations have primarily been

Further author information: (Send correspondence to D.A.K.)
D.A.K.: E-mail: dkovac@umich.edu
B.P.: E-mail: bipopa@umich.edu

Active and Passive Smart Structures and Integrated Systems XVIII, edited by Serife Tol, Guoliang Huang, Xiaopeng Li, Mostafa A. Nouh, Shima Shahab, Jinkyu Yang, Proc. of SPIE Vol. 12946, 1294606 · © 2024 SPIE · 0277-786X · doi: 10.1117/12.3009498

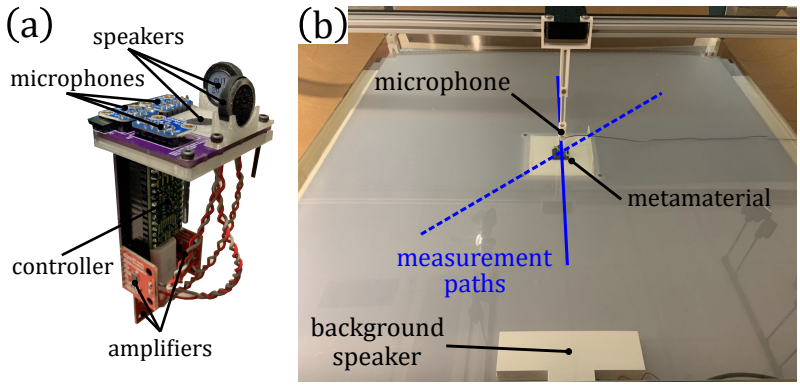

Figure 1. (a) The metamaterial unit cell consists of three microphones to sense the local field and three speakers to generate a response scaled by the controller gains. (b) The unit cell was experimentally tested in a 2D waveguide, where an external speaker provides the background field and an external microphone measures the total and scattered fields. Blue lines indicate the paths along which measurements were taken, with the solid line corresponding to trials using the pictured speaker position and dashed lines for trials with the speaker moved to the lower left corner of the waveguide.

limited to 1D operation and did not prescribe methods for implementing many cells to satisfy an arbitrary desired property map. To address this, we previously developed a polarized source model for arbitrary active acoustic metamaterial geometries in 2D that explicitly relates the programmed gains to the effective bulk modulus and mass density tensor [14]. We applied that model to an experimental metamaterial of programmable bulk modulus [15], and now in this work we expand to an experimental metamaterial of both programmable bulk modulus and mass density.

2. UNIT CELL DESIGN

We designed an active acoustic metamaterial unit cell, pictured in Fig. 1(a), with three microphones (SPH0645) as the sensing components and three speakers (AS01508MR-6-LW100-R) as the driving components. The cell is composed of two printed circuit boards (PCBs). The active acoustic elements are mounted on the upper PCB, while the controller (Teensy® 4.0) and amplifiers (MAX98357A) are mounted on the lower PCB. The unit cell was experimentally tested in a 2D waveguide, with its upper PCB flush to the lower plate of the waveguide, as shown in Fig. 1(b). The physical structure of the unit cell does not produce scattering significant enough to impact the effective acoustic properties, so all behavior can be attributed to the active response. The goal of the active unit cell design is to produce the same scattering from an arbitrary background field as would a physical unit cell of continuous material with desired κ_{eff} and $\boldsymbol{\rho}_{\text{eff}}$.

The microphones of the unit cell are arranged in a right triangle, such that the pairs along the legs can be used to sense orthogonal local pressure gradients, which can be integrated with respect to time to find the corresponding particle velocities $u_{\text{loc},x}$ and $u_{\text{loc},y}$. The average signal from all three microphones is the local pressure p_{loc}. The speakers are oriented along three perpendicular axes, where those in the x- and y-directions produce a dipole response and the one in the z-direction produces a monopole response with the upper PCB and lower waveguide plate acting as a baffle. The microphone signals are digitally input to the microcontroller, which is programmed to calculate the sensed acoustic quantities, implement a bandpass filter, and scale the outputs with the appropriate gains for the desired effective properties. The resultant signals are digitally output to the speaker amplifiers and then speakers. The relationships between the sensed and driven quantities are,

$$A^{(m)} = g^{(m)} p_{\text{loc}}, \quad A_x^{(d)} = g_x^{(d)} u_{\text{loc},x}, \quad A_y^{(d)} = g_y^{(d)} u_{\text{loc},y}, \tag{1}$$

where $A^{(m)}$ is the monopole amplitude, $A_x^{(d)}$ is the dipole amplitude in the x-direction, and $A_y^{(d)}$ is the dipole amplitude in the y-direction. The three corresponding gains g include both a magnitude and phase component, which depend on the desired local effective properties,

$$g^{(m)} = f_1\left(\kappa_{\text{eff}}\right), \quad g_x^{(d)} = f_2\left(\rho_{\text{eff},x}\right), \quad g_y^{(d)} = f_2\left(\rho_{\text{eff},y}\right). \tag{2}$$

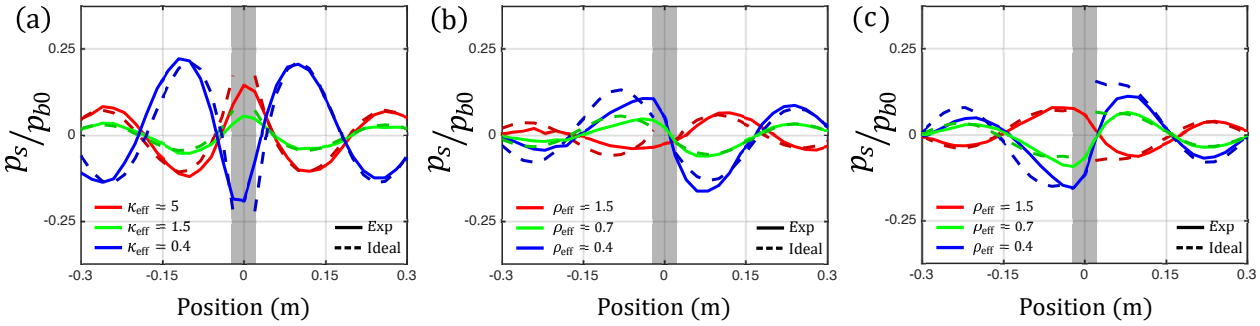

Figure 2. The experimental and ideal scattered field amplitudes at $f = 1200$ Hz are plotted by position relative to the metamaterial (indicated by a gray box) in the direction of the incident background wave. They are shown for various programmed (a) κ_{eff} and (b) $\rho_{\text{eff},y}$ with normal incidence, as well as (c) $\rho_{\text{eff},x} = \rho_{\text{eff},y}$ with incidence of 45°.

Here, the effective properties are the bulk modulus κ_{eff} and the mass density tensor components in the principle Cartesian directions $\rho_{\text{eff},x}$ and $\rho_{\text{eff},y}$. The effective properties are specified relative to the background medium, such that $\kappa_{\text{eff}} = 2$ for example signifies that the metamaterial has twice the bulk modulus of air. The relating functions f_1 and f_2 are derived in Ref. [14]. In short, the necessary gains increase in magnitude the further the desired effective properties are from those of the background medium. Also, when the desired effective properties are smaller than the background medium (fractional, closer to zero), the programmed phase of the response will be negative, while for larger than the background (approaching infinity), it will be positive.

3. EXPERIMENTAL RESULTS

We aim to experimentally demonstrate that we can program the active unit cell for a variety of κ_{eff} and $\boldsymbol{\rho}_{\text{eff}}$ by producing the ideal scattered field given some incident background field. The ideal scattered field was determined from the polarized source model of Ref. [14], which was shown to produce equivalent results to finite element method simulations of continuous media. In this work, we will consider the scattered field at a single frequency, but broadband performance can be achieved by minimizing the lag in the cell response.

For each trial, the cell was programmed for a desired effective property by adjusting the gain magnitude and delay according to Eq. (2). The cell was then ensonified by a background speaker producing a pulse at 1200 Hz with trapezoidal bounding amplitude. The speaker was positioned as shown in Fig. 1(b) for the trials with results in Fig. 2(a,b), but positioned in the lower left corner facing 45° (towards the unit cell) for those in Fig. 2(c). An external microphone on a motorized platform was used to measure the acoustic field in the propagation direction in a line of 2 cm sample spacing over 60 cm, such that half the samples were taken in the reflected region and half in the transmitted region. These measurement paths can be seen in Fig. 1(b), where the solid blue line corresponds to the Fig. 2(a,b) results and the dashed line to the Fig. 2(c) results. At each sample location, two sets of ten measurements were made and averaged, half with the cell off (background field) and half with the cell on (total field). The difference of these measurements is the scattered field p_s. The discrete Fourier transform of each time domain p_s was taken in a window of three periods in the constant amplitude region of the pulse, yielding real p_s amplitudes dependent on position.

These results are plotted in Fig. 2 relative to the background field amplitude at the cell location p_{b0}. In Fig. 2(a), the scattered fields are shown for the cell with $\kappa_{\text{eff}} = \{0.4, 1.5, 5\}$. It can be seen that the cell was producing purely monopole responses, as the scattered pressure is an even function in space. The phase of the response is inverted for κ_{eff} smaller ($\kappa_{\text{eff}} = 0.4$) and larger ($\kappa_{\text{eff}} = \{1.5, 5\}$) than the background. The amplitude of the response also increases as κ_{eff} is further from the background ($\kappa_{\text{eff}} = 1.5$ vs. $\kappa_{\text{eff}} = 5$). In Fig. 2(b), the scattered fields are shown for the cell with $\rho_{\text{eff},y} = \{0.4, 0.7, 1.5\}$. Here, the y-oriented dipole speaker of the cell was active and the scattered fields are odd functions in space. Lastly, in Fig. 2(c), the same effective densities as Fig. 2(b) are shown, but with $\rho_{\text{eff},x} = \rho_{\text{eff},y}$ and both dipole speakers active. In all three plots, the experimental

scattered fields accurately match the ideal scattered fields, indicating that the active unit cell scatters sound in the same manner as a unit cell of continuous material with the specified effective properties.

In conclusion, we demonstrated an active acoustic metamaterial of programmable bulk modulus and mass density that can be used as a building block for the fabrication of 2D devices. Only one unit cell was shown, but because its response depends just on the local field, we can extend the metamaterial to many cells, each with their own independently programmable effective properties. Additionally, the programmed $\boldsymbol{\rho}_{\text{eff}}$ of Fig. 2(c) were isotropic, but $g_x^{(d)}$ and $g_y^{(d)}$ could be set to different values for anisotropic behavior. In this way, we can potentially realize the property maps with spatial gradients and anisotropy prescribed by transformation acoustics.

ACKNOWLEDGMENTS

This work was supported by the National Science Foundation under Grant No. CMMI-1942901.

REFERENCES

[1] Cummer, S. A., Christensen, J., and Alù, A., "Controlling sound with acoustic metamaterials," *Nature Reviews Materials* **1**, 1–13 (Feb. 2016). Number: 3 Publisher: Nature Publishing Group.

[2] Liao, G., Luan, C., Wang, Z., Liu, J., Yao, X., and Fu, J., "Acoustic Metamaterials: A Review of Theories, Structures, Fabrication Approaches, and Applications," *Advanced Materials Technologies* **6**, 2000787 (Feb. 2021). Publisher: John Wiley & Sons, Ltd.

[3] Fang, N., Xi, D., Xu, J., Ambati, M., Srituravanich, W., Sun, C., and Zhang, X., "Ultrasonic metamaterials with negative modulus," *Nature Materials* **5**, 452–456 (June 2006). Number: 6 Publisher: Nature Publishing Group.

[4] Yang, Z., Mei, J., Yang, M., Chan, N. H., and Sheng, P., "Membrane-Type Acoustic Metamaterial with Negative Dynamic Mass," *Physical Review Letters* **101**, 204301 (Nov. 2008). Publisher: American Physical Society.

[5] Zhang, S., Xia, C., and Fang, N., "Broadband Acoustic Cloak for Ultrasound Waves," *Physical Review Letters* **106**, 024301 (Jan. 2011). Publisher: American Physical Society.

[6] Zigoneanu, L., Popa, B.-I., and Cummer, S. A., "Three-dimensional broadband omnidirectional acoustic ground cloak," *Nature Materials* **13**, 352–355 (Apr. 2014). Number: 4 Publisher: Nature Publishing Group.

[7] Popa, B.-I., Zigoneanu, L., and Cummer, S. A., "Tunable active acoustic metamaterials," *Physical Review B* **88**, 024303 (July 2013). Publisher: American Physical Society.

[8] Cho, C., Wen, X., Park, N., and Li, J., "Digitally virtualized atoms for acoustic metamaterials," *Nature Communications* **11**, 251 (Jan. 2020). Number: 1 Publisher: Nature Publishing Group.

[9] Akl, W. and Baz, A., "Experimental characterization of active acoustic metamaterial cell with controllable dynamic density," *Journal of Applied Physics* **112**, 084912 (Oct. 2012). Publisher: American Institute of Physics.

[10] Zhai, Y., Kwon, H.-S., and Popa, B.-I., "Active Willis metamaterials for ultracompact nonreciprocal linear acoustic devices," *Physical Review B* **99**, 220301 (June 2019). Publisher: American Physical Society.

[11] Cho, C., Wen, X., Park, N., and Li, J., "Acoustic Willis meta-atom beyond the bounds of passivity and reciprocity," *Communications Physics* **4**, 1–8 (Apr. 2021). Number: 1 Publisher: Nature Publishing Group.

[12] Chen, Y., Li, X., Nassar, H., Hu, G., and Huang, G., "A programmable metasurface for real time control of broadband elastic rays," *Smart Materials and Structures* **27**, 115011 (Oct. 2018). Publisher: IOP Publishing.

[13] Chen, Y., Li, X., Hu, G., Haberman, M. R., and Huang, G., "An active mechanical Willis meta-layer with asymmetric polarizabilities," *Nature Communications* **11**, 3681 (July 2020). Number: 1 Publisher: Nature Publishing Group.

[14] Kovacevich, D. A. and Popa, B.-I., "Transformation acoustics with bulk media composed of polarized sources," *Physical Review B* **104**, 134304 (Oct. 2021). Publisher: American Physical Society.

[15] Kovacevich, D. A. and Popa, B.-I., "Programmable bulk modulus in acoustic metamaterials composed of strongly interacting active cells," *Applied Physics Letters* **121**, 101701 (Sept. 2022). Publisher: American Institute of Physics.